Numerical and Experimental Investigations of Dusty Plasma Behavior

Pulkit Agarwal[1], Johannes Berndt[2], Eva Kovacevic[2], Adam M. Boies[1], Laifa Boufendi[2] and Steven L. Girshick[1]

[1]*Mechanical Engineering Department, University of Minnesota,111 Church St. SE, Minneapolis, Minnesota, 55455, USA, Phone/FAX: +001-612-625-5315, E-mail: slg@umn.edu*

[2]*GREMI(Group de Recherche sur l'Energetique desMilieux Ionises), CNRS/Universitie d'Orleans, 14rue d'Issoudun, 45067 Cedex 2, France*

Abstract: Numerical simulations using a 1D self-consistent plasma-aerosol model were compared to experimental measurements of a dusty argon-silane RF plasma with corresponding operating conditions. Experimental measurements were made of the spatiotemporal profiles of the intensities of laser light scattering and plasma emission. Qualitative agreement was found for several major aspects of the evolution of the emission and scattering intensity profiles.

Keywords: dusty plasmas, numerical modeling, laser light scattering

1. Introduction

Nonthermal RF plasmas in which dust particles nucleate and grow have been the subject of many experimental studies, but few comparisons exist with numerical simulations of the spatiotemporal evolution of the nanoparticle plasma system.

In the present study we investigate the spatiotemporal evolution of an argon-silane plasma from the onset of particle nucleation through particle growth, charging and transport. Experiments were performed on a capacitively coupled RF parallel plate reactor. Both plasma emission intensity and laser light scattering were measured. A 1D self-consistent plasma-aerosol model was used to calculate radiative emission from the plasma as well as laser light scattering from particles. The input parameters in the model were set insofar as possible to match the experimental conditions.

2. Approach

Numerical model

The numerical model of Warthesen and Girshick [1] as modified by Ravi and Girshick [2] was used. The plasma and aerosol phases are treated self-consistently, with the plasma treated by a fluid model while the aerosol general dynamics equation is solved using a sectional model for the particle size distribution. Effects considered include finite-rate particle charging by electron and ion attachment, particle coagulation (including the effect of image potentials on coagulation between charged and neutral particles) and particle transport by diffusion, electrostatic forces, ion drag, neutral drag and gravity. The model does not include chemistry other than electron impact ionization of argon. Nucleation and growth rates are treated as simulation parameters. The collisional-radiative model of Vlček [3] was used to calculate the emission intensity from argon at 696 nm. Laser light scattering was calculated using Mie theory, assuming spherical silicon particles with a complex refractive index equal to $5.0 + 0.1i$.

Experimental setup

The experimental setup consisted of an RF capacitive discharge with a powered upper showerhead electrode and grounded lower electrode, both with 1-mm diameter holes and 20% transparency. The discharge was not contained around the periphery of the two circular electrodes, representing an open configuration. The setup has been described in detail previously [4]. The operating conditions for experiment as well as model consist of a pressure of 17 Pa (127.5 mTorr), gas temperature 300 K, RF voltage amplitude 55 V with a DC bias at the powered electrode of -20 V, 13.56 MHz frequency and gas flow rates of 30 sccm argon and 1 sccm silane. Light scattering of particles at 90° was measured using a 405-nm laser. Plasma emission intensity was measured at 696 nm.

3. Results and discussion

The numerical model predicts the particle concentra-

tion, size distribution, and size-dependent charge distribution vs. time (following the onset of particle nucleation) at each location between the two electrodes. As shown in Fig. 1, at time t = 9 s the particle cloud has been pushed towards the lower electrode, primarily by neutral drag, and the mean particle diameter at the location of peak concentration is around 100 nm. By this time nucleation has been quenched by the expansion of the particle cloud, and coagulation has ceased, because all particles are now negatively charged.

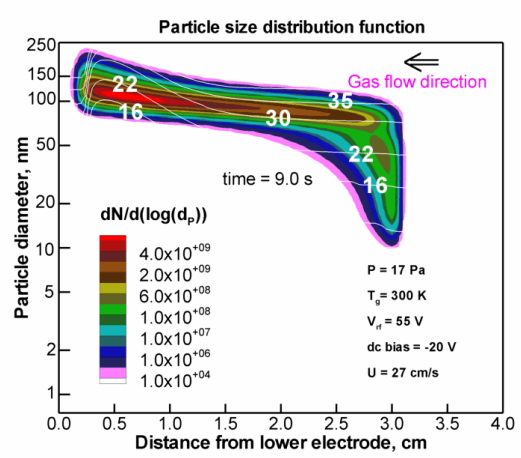

Figure 1. Simulation results for particle size distribution at 9 s following onset of nucleation. White contour lines represent average negative charge on particles.

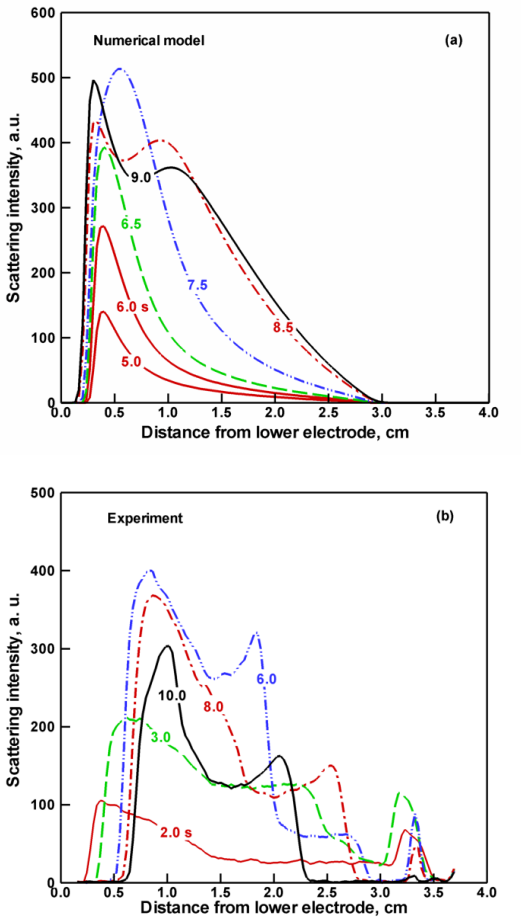

Figure 2. Particle scattering intensity vs. distance from lower electrode, from (a) numerical model and (b) experiment. Labels on the curves represent time in seconds.

Fig. 2(a) shows simulation results for predicted profiles of laser light scattering intensity at various times, and Fig. 2(b) shows the corresponding experimental measurements. Comparing these results, there are two main areas of qualitative agreement, and some discrepancies. The simulations and the experimental results both indicate that light scattering is concentrated in the lower half of the electrode gap, as expected given the strong gas drag. The simulation shows the peak in scattering located closer to the lower electrode than do the experimental results. This discrepancy has a simple explanation: the 1D model treats the lower electrode as an open grid, i.e. the model assumes constant axial velocity, whereas in the experiment the lower electrode is only partially transparent, and gas exhaust from the chamber induces a radial flow component. Hence the model overpredicts the axial velocity and gas drag near the lower electrode. Another discrepancy is that the experiments show a small scattering peak near the upper electrode, not predicted by the model. The cause of this discrepancy is presently not understood.

As seen in Fig. 2, both experimental results and simulations indicate that after several seconds the scattered intensity profile develops a double-peaked structure (not counting the small peak near the upper electrodes in the experiments), with a minimum in between. Superficially this seems to suggest the existence of a double layer of particles, one layer near the lower electrode, the other closer to the center of the plasma. However the simulation results show that this is not the case. Instead, the simulation indicates that this behavior is caused by a resonance in Mie scattering as particles grow out of the Rayleigh scattering regime and beyond about 100 nm in diameter.

This point is demonstrated by Figs. 3 and 4. Fig. 3 shows the predicted single-particle scattering intensity

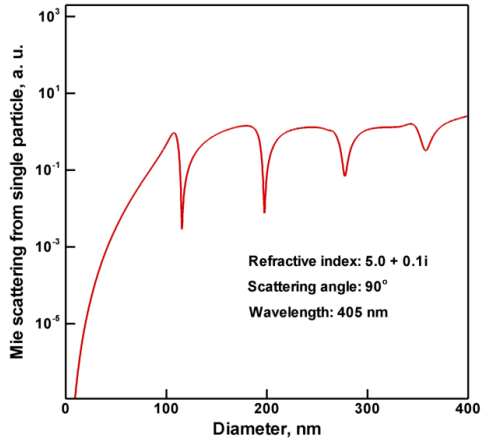

Figure 3. Scattering intensity from single particle, predicted by Mie theory. Scattering parameters given in legend.

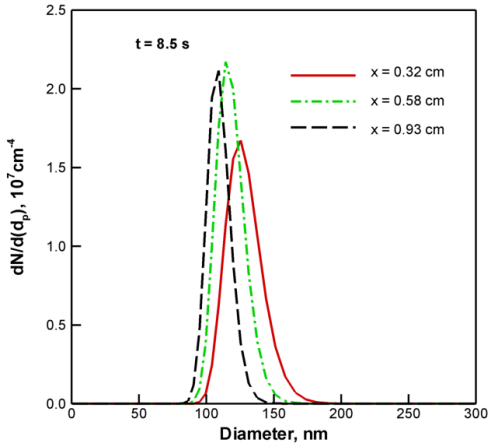

Figure 4. Particle size distributions predicted by simulation at 8.5 s, for axial locations corresponding to maxima and minimum in profile of scattering intensity.

from Mie theory. For the assumed refactive index, a first strong resonance peak (minimum in scattering) occurs at 114 nm. Fig. 4 shows particle size distributions at three locations, corresponding to the two maxima and the minimum in the scattering intensity profile in the simulation at t = 8.5 s (seen in Fig. 2a). As can be seen, the average particle size increases as distance from the lower electrode decreases. This is caused by a combination of ion drag, neutral drag and gravity. At x = 0.58 cm both the modal particle diameter and total particle concentration are higher than at x = 0.32 cm, but, as seen in Fig. 2(a), the predicted light scattering intensity is lower, because the particle size distribution at x = 0.58 cm lies right on top of the Mie resonance at 114 nm. Similarly, at x = 0.93 cm, where both the modal particle diameter and total particle concentration are lower than at x = 0.58 cm, the predicted scattering intensity is again higher.

Fig. 5 shows profiles of emission intensity at 696 nm predicted by the numerical simulation (a) and measured in the experiment (b). As can be seen, there are some similarities and some differences between the model predictions and the experiments. In both, emission intensity is relatively low in the region where particle light scattering is strongest, and peaks near the upper electrode, where light scattering is relatively weak.

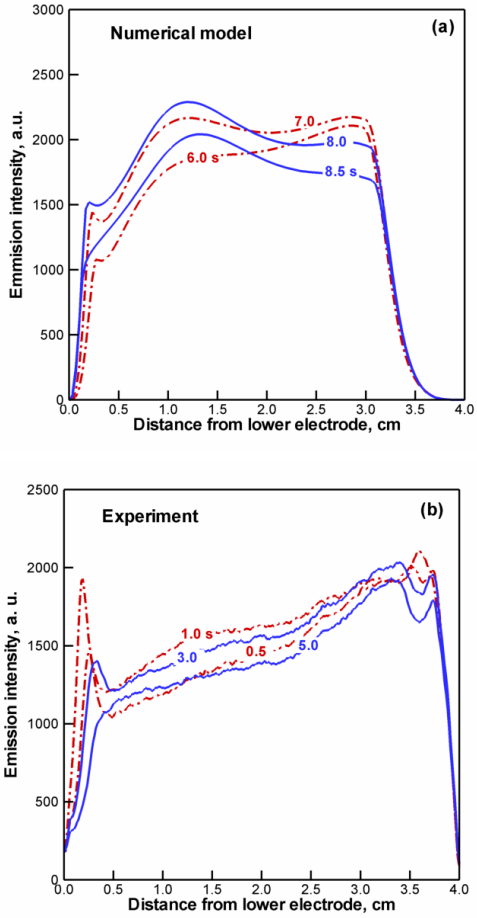

Figure 5. Profiles at various times of plasma emission intensity at 696 nm, predicted by numerical simulations (a) and measured by experiment (b).

This behavior is explained by the fact that plasma emission depends on the local electron density, and particles deplete electrons by electron attachment. This is illustrated in Fig. 6, which shows simulation results for the profiles of charge carriers at 9 s. To some extent, the emission intensity profile in Fig. 5(a) follows the electron density profile.

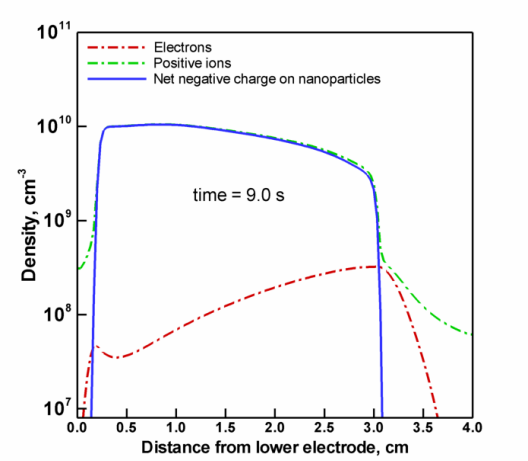

Figure 6. Predicted profiles of charge carriers at 9 s.

However the emission profile does not completely follow the electron density profile, because emission is affected not only by electron density but also by electron temperature. This fact also explains the interesting observation that both the experiment and the simulation indicate that emission intensity at first increases with time, but then begins to decrease.

For given RF voltage, as electron density decreases due to attachment to particles, electron temperature increases, maintaining ionization. This is seen in Fig. 7, where the electron temperature at the center of the plasma increases from about 1.8 eV at time zero to about 3.0 eV at 9 s. This increase in electron temperature causes emission to increase, despite the drop in electron density.

Eventually, however, the depletion of electrons in regions of high particle charge concentration becomes so strong that the frequency of ion attachment to particles

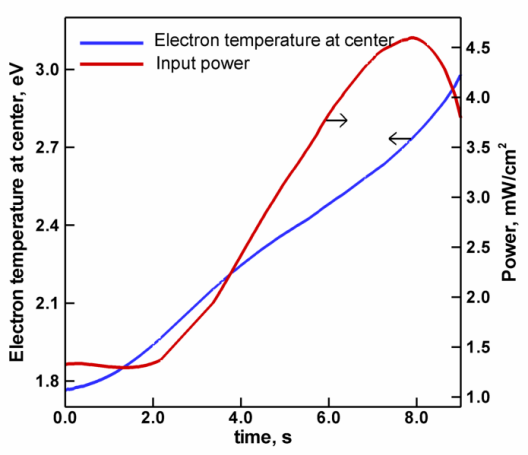

Figure 7. Electron temperature at center of discharge and power input to plasma vs. time.

can become greater than that of electron attachment. In Fig. 6, the electron density near the lower electrode sheath edge at t = 9 s is more than two orders of magnitude below the ion density. This causes the curvature in Fig. 1 in the contour lines that represent net negative charge per particle. Particles at the sheath edge carry less negative charge, on average, than particles of the same size in the center of the plasma. With less negative charge per particle, in turn the local ion density decreases, corresponding to a reduction in power input to the plasma. Finally, this causes the plasma emission to decline.

4. Summary and conclusions

Numerical simulations of the spatiotemporal evolution of an RF dusty plasma were compared to experimental measurements of plasma emission and laser light scattering. Experiment and simulation are in qualitative agreement on several major features of the evolution of the scattering and emission profiles. Some discrepancies are likey caused by the fact that the model is 1D, whereas the experimental flow profile is 3D, with the gas flow affected by the presence of an exhaust port in the bottom of the reactor, together with the open system configuration and partial transparency of the lower electrode.

5. Acknowledgments

This work was partially supported by the US National Science Foundation and (CBET-0756315) and Department of Energy (DE-SC0001939).

6. References

[1] S. J. Warthesen and S. L. Girshick, Plasma Chem. Plasma Process. **27**, 292 (2007).

[2] L. Ravi and S. L. Girshick, Physical Review E (Statistical, Nonlinear, and Soft Matter Physics) **79**, 026408 (9 pp.) (2009).

[3] J. Vlcek, J. Phys. D **22**, 623 (1989).

[4] A. Bouchoule, A. Plain, L. Boufendi, J. P. Blondeau, and C. Laure, J. Appl. Phys. **70**, 1991 (1991).